

## Effects of Chitosan Characteristics on the Physicochemical Properties, Antibacterial Activity, and Cytotoxicity of Chitosan/2-Glycerophosphate/Nanosilver Hydrogels

Hsiang-Wei Chang, Ya-Shen Lin, Ying-Die Tsai, Min-Lang Tsai

Department of Food Science, National Taiwan Ocean University, Keelung 20224, Taiwan, Republic of China

Correspondence to: M.-L. Tsai (E-mail: tml@mail.ntou.edu.tw)

**ABSTRACT:** The effects of molecular weight (MW) and the degree of deacetylation (DD) of chitosan (CS) on the physicochemical properties, antibacterial activity, and cytotoxicity of CS/2-glycerophosphate (GP)/nanosilver hydrogel in the development of a thermo-sensitive *in situ* formed wound dressing are examined herein. The gelation temperatures for the hydrogels were measured in the range of 32–37°C by manipulating the MW and DD of CS and the GP concentration. The structure of 88% DD CS hydrogel was more porous, uniform, and connective than that of the 80% DD CS hydrogel. The superior water vapor transmission rates of hydrogels with 80% and 88% DD CS were  $7150 \pm 52$  and  $9044 \pm 221 \text{ gm}^{-2} \text{ d}^{-1}$ , respectively. The skin permeations of nanosilver by the 80% and 88% DD CS hydrogels were 3.82 and 4.99  $\mu\text{g cm}^{-2}$ , respectively, in 24 h tests. Both the hydrogels with 6 and 12 ppm nanosilver showed cytotoxicity for HS68 cells. The diameters of the hydrogel's inhibition zones for *Pseudomonas aeruginosa* and *Staphylococcus aureus* increased when the concentration of nanosilver increased and the MW of the CS decreased. Therefore, the hydrogel could be prepared with lower MW CS and lower concentration of nanosilver in order to reduce the cytotoxicity of nanosilver, while maintaining similar antibacterial activity for a hydrogel prepared with higher concentration nanosilver and higher MW CS. © 2012 Wiley Periodicals, Inc. *J. Appl. Polym. Sci.* 000: 000–000, 2012

**KEYWORDS:** chitosan/2-glycerophosphate hydrogel; nanosilver; degree of deacetylation; molecular weight; cytotoxicity; antimicrobial

Received 12 July 2011; accepted 6 April 2012; published online

DOI: 10.1002/app.37855

### INTRODUCTION

Chitosan (CS) is a linear polysaccharide linked by a  $\beta$ -1,4 glycoside, and composed of *N*-acetyl-D-glucosamine and D-glucosamine. It is the most widespread polycationic biopolymer; it is abundant in nature, nontoxic, biocompatible, and biodegradable. It is commercially used in foods, agriculture, biochemistry, wastewater treatment, paper, textiles, cosmetics, nanoparticles, hydrogels, liquid crystals, membranes, and microcapsules.<sup>1,2</sup> Chitin and CS (deacetylated chitin) are also used in medical applications, such as in drug delivery systems, tissue scaffolds, wound dressing, biosensors, separation membranes, and antibacterial coatings.<sup>3–9</sup>

The CS/glycerophosphate (CS/GP) solution in the physiological pH range converts into a gel state when heated to body temperature level.<sup>10</sup> A number of works have reported on CS/GP hydrogel's biomedical applications, such as drug delivery systems, tissue engineering, and cancer treatment.<sup>10–16</sup> The gelation mechanism of CS/GP hydrogel may operate by changing from a pH-dependent status to a thermal-pH dependence. At low tem-

peratures, GP can increase the pH of CS solutions to around neutrality. It might screen the electrostatic repulsion between CSs and theoretically lead to gelation because it is pH-induced. However, due to attraction between the phosphate moieties of GP and  $-\text{NH}_3^+$  groups of CS, hydroxyl groups of GP could increase the stability and hydrophilicity in CS, as well as maintain its solubility at low temperatures for a period of time. When the temperature increases, it reduces the polarity of the CS, and the glycerol moiety of GP increases the hydrophobicity, causing CS dehydration and increased interchain hydrophobic attraction.  $\text{H}^+$  was removed from  $-\text{NH}_3^+$  and was accepted by  $-\text{PO}_4^{2-}$ , thereby further reducing both the CS charge density and the attraction of CS and GP. This reaction allowed hydrophobic and hydrogen bonding between the CSs to predominate; and upon the heating of the CS/GP solution, a hydrogel was formed.<sup>10–12,17,18</sup>

The physicochemical properties of CSs depend on such intrinsic factors as the degree of deacetylation (DD), the distribution of acetyl groups, molecular weight (MW) and polydispersity.<sup>19</sup> The

© 2012 Wiley Periodicals, Inc.

MW and DD of CS affect the rheological property, chain flexibility, mechanical properties, and pore size of the membrane and microcapsules. They also affect the water-retention capacity of cosmetics, antimicrobial activity, and immunoadjuvant reaction, as well as the enzyme and metal-binding abilities.<sup>20</sup> The DD and MW, as important characteristics of CS, affect such properties of CS/GP hydrogel as the gelation temperature, gelation rate, viscosity, biological compatibility, and drug delivery properties.<sup>21–23</sup>

Nanosilver has been used for a long time as an antimicrobial agent. The typical minimum inhibitory concentration (MIC) and minimum bactericidal concentration (BMC) of nanosilver against standard reference cultures are 1.56–6.25 ppm and 12.5 ppm, respectively.<sup>24</sup> Chitin or CS-based wound dressings containing nanosilver have been developed.<sup>8,9,25</sup> Sudheesh Kumar et al.<sup>9</sup> reported that  $\beta$ -chitin/nanosilver composite scaffolds were bactericidal against *Escherichia coli* and *Staphylococcus aureus*. The scaffolds also showed good blood clotting ability and good attachment to vero cells. However, results from Madhumathi et al.<sup>8</sup> and Ong et al.<sup>25</sup> showed cytotoxicity *in vitro* for chitin or CS/nanosilver dressing.

The MW and DD should affect the properties of CS/GP hydrogel since CS is the major component of this hydrogel. The addition of nanosilver will insignificantly affect the gelation temperature of CS/GP hydrogel<sup>23</sup>; however, while it may improve the antibacterial activity of the hydrogel, it also increases the cytotoxicity. Therefore, this study focuses on investigating the effects of the DD and MW of CS and the concentration of nanosilver on the physicochemical properties, antibacterial activity, and cytotoxicity of CS/2-glycerophosphate/nanosilver (CS/GP/Ag) hydrogels. The feasibility evaluation of this hydrogel system aims to develop a thermosensitive, *in situ* formed wound dressing to fit any irregular-shape and -size wounds.

## MATERIALS AND METHODS

### Materials

In this study, CSs were used with 80% DD (DD80) and different MWs (145, 161, and 335 kDa) and with 88% DD (DD88) and different MWs (113, 146, 160, and 204 kDa). The preparation method was described by Tsai et al.<sup>23</sup> The DD and MW of these CSs were determined with infrared spectrometry and size exclusion high performance liquid chromatography, respectively.<sup>23</sup> Silver nitrate, sodium borohydride, GP (2-glycerophosphate, disodium salt, pentahydrate), acetic acid, sodium acetate, sodium azide and sodium chloride were purchased from the Sigma-Aldrich Co. (MO). Hydrochloric acid and sodium hydroxide were purchased from Merck & Co., (Darmstadt, Germany). GIBCO<sup>®</sup> Dulbecco's phosphate buffered saline was purchased from the Invitrogen Co. (NY). Dulbecco's Modified Eagle Media (DMEM) was purchased from Hyclone (UT). Nutrient agar and nutrient broth were purchased from Becton Dickinson (MD). Dimethyl sulfoxide was purchased from Panreac (Barcelona, Spain). *S. aureus* BCRC 10780 and *Pseudomonas aeruginosa* BCRC 10944 were provided by Bioresource Collection and Research Center (FIRDI, Hsinchu, Taiwan). HS68 human epidermis fibroblast cells were provided by the National Health Research Institutes (NHRI) Cell Bank (Taipei, Taiwan).

### Preparation of Thermosensitive Hydrogel

After 30 mL of 0.002M sodium borohydride solution was chilled in an ice bath for 20 min, 6 mL of 0.001M silver nitrate solution was added dropwise to the sodium borohydride solution. As a result of the chemical reaction, pale yellow nanosilver formed. The prepared nanosilver solution was characterized by ultraviolet–visible spectrophotometry<sup>9</sup> (Hitachi, U-2800A, Tokyo, Japan). CS (200 mg) was dissolved in 1% (v/v) aqueous acetic acid (9 mL) to prepare a CS solution. GP (200–700 mg) was dissolved in distilled water (1 mL) to prepare GP solutions. After chilling the CS and GP solutions at 4°C for 1 h, they were mixed and stirred for 2 min in an ice bath. Next, the hydrogel solution was shaken for 40 s by a vortex shaker. The resulting hydrogel solution contained 2% (w/v) CS and 2–7% (w/v) GP, and the pH value of the solution was adjusted to 6.5. Nanosilver solution (6 or 12 ppm) was added to the hydrogel solution and mixed using a vortex shaker.<sup>23</sup> The concentration and size of the nanosilver were determined by an atomic absorption spectrophotometer (Perkin-Elmer 510 OPC, Norwalk, CT) and a transmission electron microscope (TEM, JEOL, JEM 1230, Tokyo, Japan), respectively.

### Determination of Viscosity

Initially, 1 mL of the hydrogel solution was poured into the MK21 cone/plate of a rheometer (Rheolab, Paar Physica MC 120, Stuttgart, Germany). The shear rate was adjusted to 100 s<sup>-1</sup>, and the viscosity of the hydrogel solution was measured while increasing the temperature at a rate of 1°C min<sup>-1</sup> during the heating process.<sup>17</sup>

### Examination of Microstructures

The porous structure of CS/GP/Ag hydrogel was examined using a scanning electron microscope (SEM, Hitachi S-4800, Tokyo, Japan). To prepare the SEM samples, we heated a perfect solution to gelation temperature for 1 h and dipped it into a handful of liquid nitrogen to quick freeze the structure. Carbon gels, with an adequate area adhering to the operating table, were selected to carry the quick frozen hydrogels to be dried with a freeze-drier for 48 h afterward, and these carbon gels were then coated with a layer of gold using an ion-membrane depositor (Hitachi, E-1010, Tokyo, Japan) for examination of the hydrogel microstructure.

### Determination of Water Vapor Transmission Rate

A modified ASTM standard method (inverted cup, E96-90) was used to determine the water vapor transmission rate (WVTR) of CS/GP/Ag hydrogel. Fifteen grams of pure water was poured into a cylindrical container with a bottom area of 17.35 cm<sup>2</sup> and a height of 3.7 cm, and this was covered by pregelation hydrogel to a thickness of 2 mm. The container was placed within a Temperature/Humidity Test Chamber (Terchy Tech. Ltd., HRM-80FA, Nantou, Taiwan) with the temperature and humidity set at 36.5 ± 1.5°C and 32 ± 5%, respectively. The amount that the water weight decreased was determined during a period of 6 h. The WVTR was calculated by the following equation<sup>26</sup>:

$$\text{WVTR}(\text{gm}^{-2}\text{d}^{-1}) = (m/t) \times (24/A)$$

where  $m$  is the decrease in water weight (g),  $t$  is the measured time (h), and  $A$  is the covered surface area (m<sup>2</sup>).

### Measurement of Skin Permeation

The permeability of silver ions through a BALB/c mouse's skin was investigated using Franz Diffusion Cells with an effective

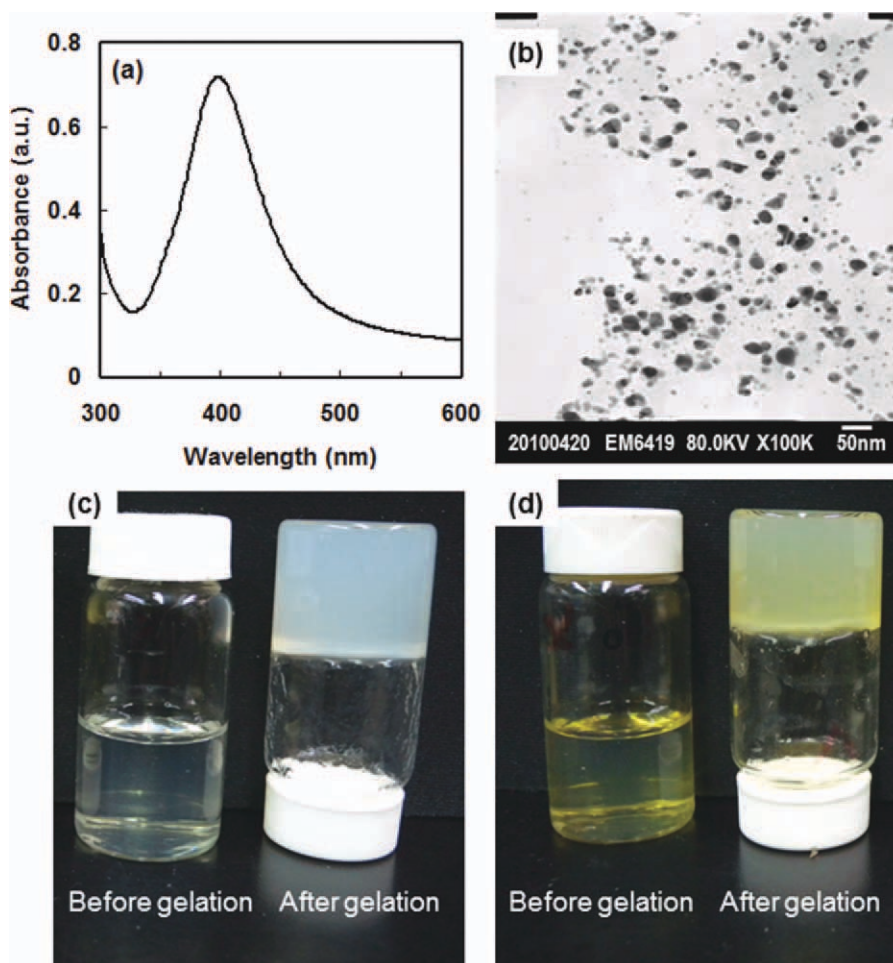


**Figure 1.** (a) UV-vis absorption spectrum; (b) transmission electron microscopic photograph of nanosilver. Photograph of CS/GP thermosensitive hydrogel solution (c) without nanosilver and (d) with nanosilver. [Color figure can be viewed in the online issue, which is available at [wileyonlinelibrary.com](http://wileyonlinelibrary.com).]

diffusional area of  $0.785 \text{ cm}^2$ . The hair on the mice skins was removed. The skins were excised and then clamped between the donor and the receptor chamber with 5.6 mL cell volume. The receptor chamber was filled with a phosphate buffer to ensure sink conditions. The receptor chamber was thermostatically controlled at  $37^\circ\text{C}$  and the solution was stirred continuously at 300 rpm. One milliliter of CS/GP hydrogel containing 20.22 ppm of nanosilver was pipetted into each donor compartment and sealed with paraffin to prevent evaporation. Samples (1 mL) from the acceptor medium were drawn at different time intervals from the acceptor compartment and immediately replaced with 1 mL of the phosphate buffer.<sup>27</sup> The silver concentration of the sample was determined using an atomic absorption spectrophotometer (Perkin-Elmer 510 OPC, Norwalk, CT). The permeation amount of the nanosilver was calculated with the above silver concentration.

#### Examination of Cytotoxicity

HS68 human fibroblast cells were cultured in a DMEM media supplemented with 2.2 g/L sodium bicarbonate and 10% fetal bovine serum (FBS). Cells were subcultured according to ATCC recommendations without using any antibiotic. In order to examine the cytotoxicity, cells were seeded on CS/GP/Ag hydrogel on 48-

well plates at  $5 \times 10^4$  cells per well. Cell viabilities were determined at 0, 12, and 48 h. For each time point, 50  $\mu\text{L}$  of mammalian cell solution from a LIVE/DEAD<sup>®</sup> Viability/Cytotoxicity Kit was added to the culture medium, and monolayer cultured cells were used as a control sample. The samples were incubated at  $37^\circ\text{C}$  for 30 min. After washing the samples three times with PBS, the stained cells were examined using fluorescence microscopy (Olympus, BX-51, Japan).

#### Antibacterial Activity

*S. aureus* and *P. aeruginosa* were used to assay the antibacterial activity of CS/GP/Ag hydrogel using the modified Kirby-Bauer Disc Diffusion Method. These bacteria were grown overnight in nutrient broth. Fifty microliters of hydrogel solution was placed on filter paper (8 mm). Then the paper was placed in a nutrient agar of *S. aureus* ( $10^6$  CFU/mL) and *P. aeruginosa* ( $10^6$  CFU/mL). All of the samples were cultured at  $37^\circ\text{C}$  for 24 h. Finally, the sizes of the antibacterial circles were measured.<sup>9</sup>

#### Statistical Analysis

All of the data were analyzed by a One-Way Analysis of Variance (ANOVA). When the One-Way ANOVA identified differences among the groups, multiple comparisons among the means were

made using Duncan's New Multiple Range Test. Statistical significance was determined by setting the aggregate Type I error at 5% ( $P < 0.05$ ) for each set of comparisons, using an SPSS computer program (version 12.0) for Windows. Only the WVTR data were analyzed by the Student's *t*-test for comparison of the control and treatment groups.

## RESULTS AND DISCUSSION

### Characterization of Nanosilver

Figure 1(a) shows the UV-visible absorption spectrum of the prepared nanosilver solution, which reveals a broad adsorption peak at 400 nm. The broad plasmon absorption peak at 400 nm is characteristic of small sized nanosilver particles.<sup>9,24,28</sup> Figure 1(b) shows a TEM photograph of the nanosilver. The average size of the nanosilver particles was 21.8 nm, which was calculated with image analysis software. These results confirm that the silver particles were nanometer sized. Figure 1(c, d) shows the photographs of CS/GP and CS/GP/Ag hydrogels, respectively. The CS/GP/Ag hydrogel appears pale yellow due to the addition of nanosilver. Obviously, the color appears different between the CS/GP hydrogel and CS/GP/Ag hydrogel.

### Viscosity of Hydrogel

Figure 2 shows the viscosity changes of CS/GP/Ag hydrogel solutions as a function of temperature, determined at a temperature increase rate of  $1^\circ\text{C min}^{-1}$ , in which the shear rate was adjusted to  $100\text{ s}^{-1}$ . When the temperature rose to  $32^\circ\text{C}$ , the hydrogel viscosity of CS samples with an 80% DD and 161 kDa MW (DD80/MW161) and samples with 88% DD and 160 kDa MW (DD88/MW160) did not significantly change. At this time,

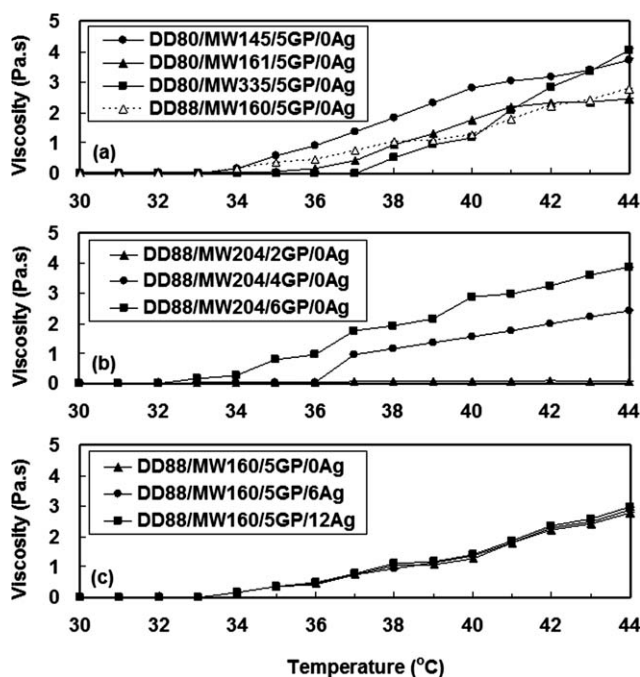


**Figure 2.** The viscosities of CS/GP/Ag hydrogels as a function of temperature determined at a shear rate of  $100\text{ s}^{-1}$ . DD80/MW145/5GP/0Ag expressed the hydrogel prepared with 80% DD and 145 kDa CS, 5% GP, and 0 ppm nanosilver. The rest may be deduced by analogy.

the hydrogels were still in solution [Figure 2(a)]. When the temperature increased to  $34^\circ\text{C}$ , the viscosity of the DD88/MW160 hydrogel sample increased significantly. This temperature is the gelation temperature at which time the sol-gel transition and a significant increase in viscosity occurred. The increase in viscosity for CS samples of DD80/MW161 hydrogel began at  $36^\circ\text{C}$ , indicating that hydrogel prepared with a higher CS DD had a lower gelation temperature. CS with a higher DD, which had more amine groups, could form more crosslinks with the GP phosphate group. This process led to an increase in the gelation rate and, consequently, decreased the gelation temperature.<sup>10,12</sup> Similar results were reported by Tsai et al.<sup>23</sup> They proposed that a higher DD CS chain was more flexible, making a change of the original conformation in the sol-gel process easier and resulting in a lower gelation temperature. However, Zhou et al.<sup>22</sup> reported that the viscosity of CS/GP hydrogel prepared with a CS having a DD of 75.4%, increased quickly to  $37^\circ\text{C}$ , while others increased more slowly. The optimal DD for a prepared hydrogel was found to be 75.4%.

Figure 2(a) also reveals that the gelation temperatures of hydrogels prepared using DD88 CSs with MWs of 145, 161, and 335 kDa were 34, 36, and  $38^\circ\text{C}$ , respectively; this means that the gelation temperature increases with the increase in the CS's MW. A CS with a higher MW has a larger hydrodynamic volume, which makes it more difficult to change the original conformation in the sol-gel process, resulting in a higher gelation temperature. Besides, CS with a higher MW has fewer exposed  $-\text{NH}_3^+$  groups due to its more compact conformation,<sup>29</sup> leading to the ratio of attraction between the CS and GP being smaller than CS with a lower MW; this reaction makes the sol-gel transition more difficult and creates a higher gelation temperature. Furthermore, the trend of CS hydrogel samples' viscosity to increase with MWs of 145 and 161 kDa was similar because of their close MW levels. However, the trend of viscosity increase for CS hydrogel with an MW of 335 kDa was greater than that of samples with MWs of 145 and 161 kDa, indicating that the mechanical properties of hydrogel are better when prepared with a larger MW CS.

Figure 2(b) exhibits that the gelation temperature of hydrogel decreases with increasing concentrations of GP. The viscosity of hydrogel with 6% (w/v) GP increased significantly at  $33^\circ\text{C}$  and was insignificantly affected by constant shear force when heated, illustrating that this hydrogel has greater mechanical strength. The viscosity of hydrogel containing 4% (w/v) GP increased significantly at  $37^\circ\text{C}$ . However, the viscosity of hydrogel with 2% (w/v) GP had an insignificant increase even when heated to  $50^\circ\text{C}$ , retaining its solution state during the entire time. Chenite et al.<sup>17</sup> found that the gelation temperature of hydrogel decreased with increasing GP concentrations because of the decreasing charge density of CS at higher GP concentrations, along with easier sol-gel transition. Tsai et al.<sup>23</sup> found that CS has a lower charge density and higher chain flexibility at a higher GP concentration, causing CS chains to be closer to each other, to entangle more easily and to make gel.

Figure 2(c) shows that the gelation temperature of CS/GP hydrogels with different concentrations of nanosilver (0, 6, and

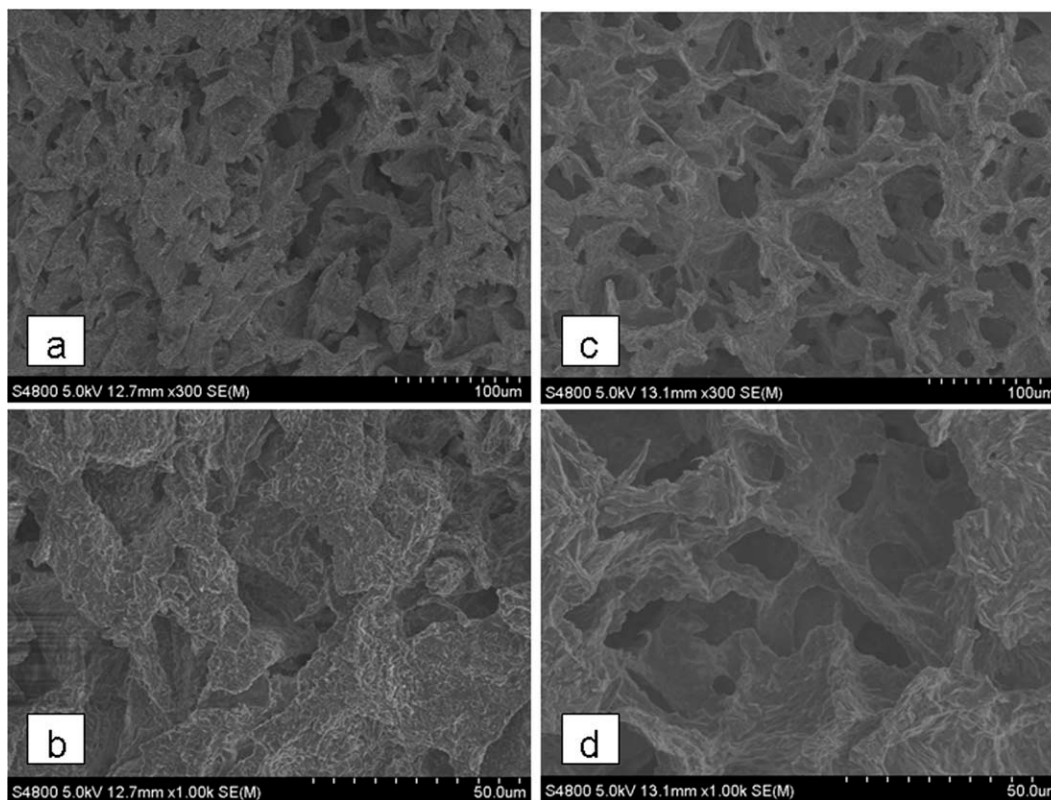


**Figure 3.** SEM micrographs of CS/5% GP/Ag hydrogels, (a) DD80/MW161 300 $\times$ , (b) DD80/MW161 1000 $\times$ , (c) DD88/MW160 300 $\times$ , (d) DD88/MW160 1000 $\times$ .

12 ppm) was 34 $^{\circ}$ C for all of them. The viscosities of hydrogels with 0, 6, and 12 ppm nanosilver were insignificantly affected by the concentration of nanosilver. The results indicate that the effect of the addition of different concentrations of nanosilver on the gelation temperature and viscosity of CS/GP/Ag hydrogel is insignificant, perhaps due to the fact that the amount of nanosilver is very low compared to the CS and GP.

Factors such as the MW and DD of the CS and the concentration of GP can be controlled, leading to the gelation temperature being close to body temperature (32–37 $^{\circ}$ C) and forming a gel *in situ* by body heat.

#### Microstructure of Hydrogel

Figure 3 shows the microstructure of cross-sections of lyophilized CS/GP/Ag hydrogels prepared with DD80 and DD88 CS samples as the two types of hydrogels. The structure of DD88 CS hydrogel was more porous, uniform, and connective than that of the DD80 CS hydrogel. The DD88 CS hydrogel's superior porosity may be the result of a higher DD of the CS, which makes the hydrogel more flexible and compact when forming larger and more porous structures.<sup>30–32</sup>

#### Water Vapor Transmission Rate of Hydrogel

Figure 4 shows the WVTR of CS/GP/Ag hydrogels prepared with DD80 and DD88 CS samples (MW of the CS was about 160 kDa). The results indicate that the superior WVTR values of the DD80 and DD88 hydrogels were 7150  $\pm$  52 and 9044  $\pm$  221  $\text{gm}^{-2} \text{d}^{-1}$ , respectively. The WVTR of DD88 hydrogel was

larger than that of DD80 hydrogel, perhaps due to the higher DD of the CS making it more flexible and compact to form larger and more porous structures.<sup>30–32</sup> As a result, vapor is more easily released from the hydrogel. The results correspond to those in Figure 3.

An essential requisite for a wound dressing is that it possesses a suitable WVTR.<sup>26</sup> An ideal dressing would control the water evaporation at an optimal rate to prevent the accumulation of excessive exudate, while ensuring that wound dehydration does

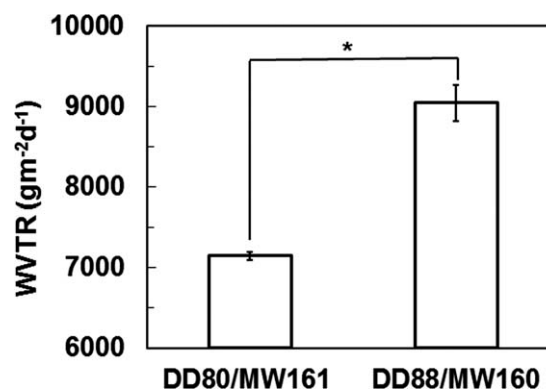


**Figure 4.** Water vapor transmission rates (WVTR) of CS/5% GP/Ag hydrogels based on different degrees of deacetylation of CS. Each value represents mean  $\pm$  S.D. ( $n = 3$ ). \* Statistical significance with  $P < 0.05$ .

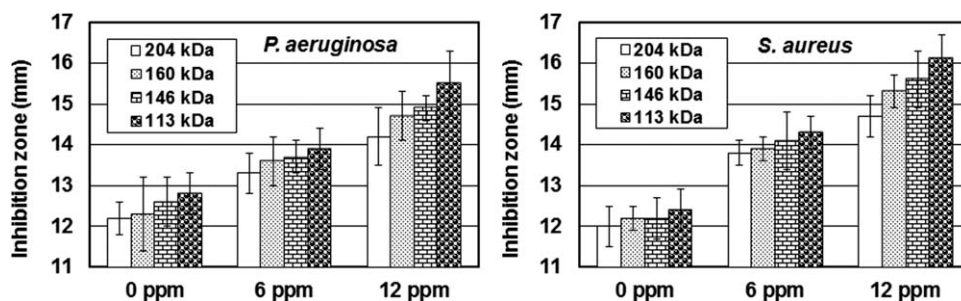


**Figure 5.** Effects of concentration of nanosilver and MW of CS on the inhibition zones (mm) for DD88 CS/5% GP/Ag hydrogels. Values are mean  $\pm$  S.D. ( $n = 10$ ).

not occur.<sup>33</sup> The evaporative water loss for normal skin is  $204 \pm 12 \text{ gm}^{-2} \text{ d}^{-1}$ , while that for injured skin could range from  $279 \pm 26 \text{ gm}^{-2} \text{ d}^{-1}$  for a first-degree burn to  $5138 \pm 220 \text{ gm}^{-2} \text{ d}^{-1}$  for a granulating wound.<sup>34</sup> It has been recommended that a rate of  $2000\text{--}2500 \text{ gm}^{-2} \text{ d}^{-1}$ , which is in the midrange of loss rates from injured skin, would provide an adequate level of moisture without risking wound dehydration.<sup>33</sup> The water vapor loss from exposed skin wounds mainly depends on the wound depth.<sup>35</sup> Thus, it can be seen that both the DD80 and DD88 hydrogels with superior WVTRs may be suitable for wounds with more exudates, as well as for ulcers.

#### Antimicrobial Activity of Hydrogel

Figure 5 shows the diameters of inhibition zones against *S. aureus* and *P. aeruginosa* for DD88 CS/GP hydrogels with different MWs (113, 146, 160, and 204 kDa) and containing different concentrations of nanosilver (0, 6, and 12 ppm). The results indicate that all of the diameters of the hydrogel inhibition zones for *P. aeruginosa* and *S. aureus* increased as the concentration of nanosilver increased. These results are similar to those observed by Sudheesh Kumar et al.,<sup>9</sup> which showed that the diameters of the inhibition zones of  $\beta$ -chitin/nanosilver scaffolds plotted against *S. aureus* and *E. coli* increased with increasing nanosilver concentration. Jain et al.<sup>24</sup> indicated that the MIC<sub>50</sub>, MIC<sub>90</sub>, and MBC<sub>99.9</sub> of nanosilver for *P. aeruginosa* were 3.12, 6.25, and 12.5 ppm, respectively, and the MIC<sub>50</sub> and MIC<sub>90</sub> for *S. aureus* were 6.25 and 12.5 ppm, respectively. It may be necessary for this hydrogel system to contain 6–12 ppm of nanosilver to ensure good antibacterial activity regardless of other factors.

Figure 5 also shows that the diameters of the hydrogel inhibition zones for *P. aeruginosa* and *S. aureus* increased when the CS's MW decreased. This may be due to a lower MW CS have higher pKa and more protonation.<sup>36</sup> The diameters of hydrogel prepared with 204 kDa CS and containing 12 ppm of nanosilver were  $14.2 \pm 0.7$  and  $14.7 \pm 0.5$  for *P. aeruginosa* and *S. aureus*, respectively. They are similar to that of the hydrogel prepared with 113 kDa CS and containing 6 ppm, which were  $13.9 \pm 0.5$  and  $14.3 \pm 0.4$  for *P. aeruginosa* and *S. aureus*, respectively. Therefore, in order to reduce the cytotoxicity of nanosilver and obtain similar antibacterial activity, the hydrogel could be prepared with a lower MW CS and a lower concentration of nanosilver.

Figure 5 shows that the antibacterial activity of hydrogel without nanosilver for *P. aeruginosa* (Gram-negative) was better than that for *S. aureus* (Gram-positive), perhaps because of the

different structures and compositions of the Gram-negative and Gram-positive cell walls. The major constituent of a Gram-positive bacteria cell wall is peptidoglycan, with a small amount of protein. The cell walls of Gram-negative bacteria, on the other hand, are thinner and contain more complex and varied polysaccharides, proteins and phospholipids, in addition to the peptidoglycan.<sup>37</sup> The peptidoglycan has a positive charge, while the phospholipid has a negative charge. The positively charged CS amino group can easily interact with the negatively charged phospholipid of Gram-negative bacteria, thus altering the cell membrane structure and resulting in changes to the cell membrane permeability, as well as allowing more intracellular substances to leak out. Therefore, the antibacterial activity of CS for Gram-negative bacteria is better than that for Gram-positive bacteria.

#### Cytotoxicity of Hydrogel

Figure 6 indicates that the cell viabilities of HS68 human fibroblast cells incorporated in CS/GP hydrogels with different GP concentrations and CS MWs without nanosilver after 12 h were in the range of 77.9–87.9%. CS is a nontoxic, biocompatible, and biodegradable polysaccharide.<sup>1</sup> GP has been approved by the FDA for venous administration.<sup>13</sup> The material shows no cytotoxicity if the relative generative rate is greater than 75%.<sup>38</sup> Zhao et al.<sup>39</sup> reported that CS/GP systems prepared by dissolving CS in tested acids, except for chloroacetic acid, were nontoxic to mouse embryonic fibroblasts and Hela cells. Consequently, the CS/GP hydrogels showed no cytotoxicity for HS68 cells. However, the cell viability of HS68 cells seeded in CS/GP hydrogels with 6 and 12 ppm of nanosilver after 12 h was in the range of 47.7–61.3% and 22.7–33.3%, respectively, and showed cytotoxicity for normal human cells. These HS68 cells keep on culturing for 48 h and cell viability recovered to 51.9–69.7% and 49.2–59.0% for 6 and 12 ppm nanosilver hydrogel, respectively. The results are similar to the cytotoxicity of silver-load CS/polyphosphate dressing for Neonatal Human Dermal Fibroblasts.<sup>25</sup>

Sudheesh Kumar et al.<sup>9</sup> reported that  $\beta$ -chitin scaffolds containing 0.001–0.006% nanosilver were noncytotoxic to vero cells. However, Madhumathi et al.<sup>8</sup> indicated that chitin scaffolds loading 0.003–0.005% nanosilver were cytotoxic to L929 mouse fibroblasts. Ong et al.<sup>25</sup> showed that CS/polyphosphate/silver dressing was severely cytotoxic to Neonatal Human Dermal Fibroblasts. Cytotoxicity of the CS/silver composite was due to nanosilver present in these systems.<sup>8,25</sup> The cytotoxicity of

nanosilver depends on doses of exposure, surface coating, and the degree of agglomeration, i.e., the cytotoxicity increases as nanosilver concentration increases and the cytotoxicity decreases as the agglomeration degree of nanosilver increases, due to agglomeration limiting surface availability and access to membrane bound organelles; surface coating of nanosilver may increase or decrease cytotoxicity depending on the coating material.<sup>40</sup> The cytotoxicity results of nanosilver loading chitin or CS-based hydrogel, including references<sup>8,9,25</sup> and our results, are discrepant. The above factors may be the cause. Additionally, Ong et al.<sup>25</sup> reported that the wound healing was satisfactory on a murine model and showed good fibroblast proliferation and keratinocyte maturation in the epidermis. The conflict between *in vitro* and *in vivo* results may be due to silver ions being rapidly inactivated by chloride and protein in the wound.<sup>8</sup>

#### *In Vitro* Skin Permeation Studies

Figure 7 shows the time-course profile of nanosilver permeation from CS/GP/Ag hydrogel through mouse skin. The size and initial concentration of the nanosilver were 21.8 nm and 20.22 ppm (25.76  $\mu\text{g}/\text{cm}^2$ ), respectively. The results show that the permeation amounts of nanosilver from DD80 and DD88 CS hydrogels were 3.82 (14.8%) and 4.99  $\mu\text{g}/\text{cm}^2$  (19.4%), respectively on BALB/c mouse skin after 24 h. The results correspond to the results of SEM and WVTR examinations. The three-dimensional network of DD88 CS hydrogel had a more porous structure, which favors nanosilver permeation. Laresse et al.<sup>41</sup> reported that the permeation amounts of nanosilver were 0.46 and 2.32  $\text{ng}/\text{cm}^2$ , respectively, when filled with 70  $\mu\text{g}/\text{cm}^2$  and 25 nm of nanosilver coated with polyvinylpyrrolidone through

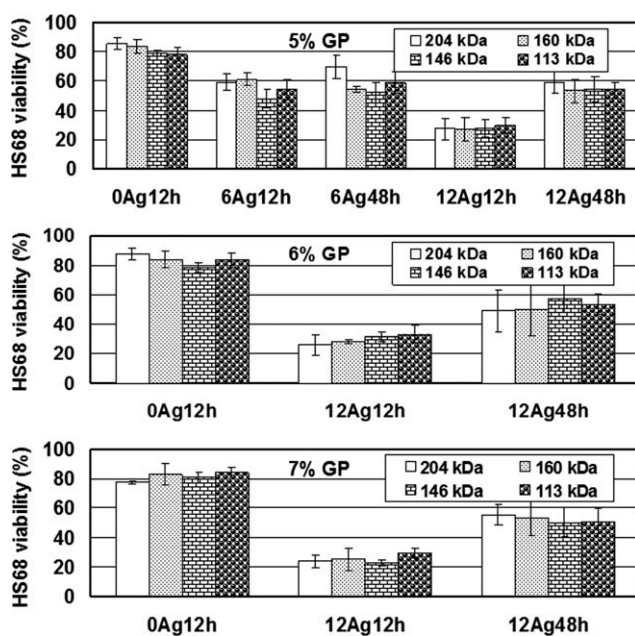


**Figure 6.** Effects of concentration of GP, MW of CS, nanosilver concentration, and culture time on the viability of HS68 epidermis fibroblasts incorporated in DD88 CS/GP/Ag hydrogels. Cell density:  $5 \times 10^4$  cells/well. 12Ag12h expressed the hydrogel containing 12 ppm nanosilver and cultivated for 12 h. The rest may be deduced by analogy. Values are mean  $\pm$  S.D. ( $n = 3$ ).

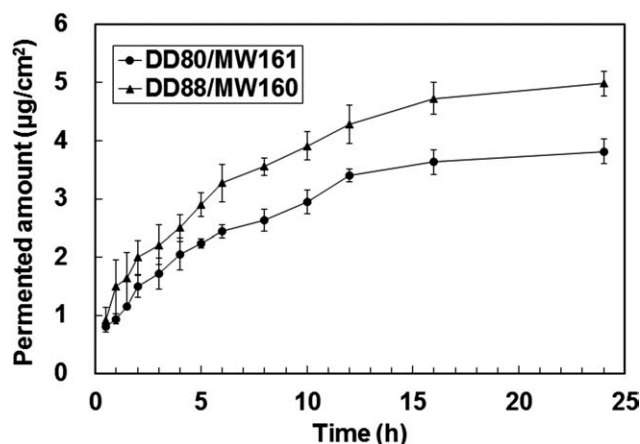


**Figure 7.** Time-course profiles of nanosilver permeation of CS/5% GP/Ag hydrogels through mouse skin. The initial concentration of nanosilver was 20.22 ppm. Each value represents mean  $\pm$  S.D. ( $n = 3$ ).

intact and damaged human skin after 24 h. The permeation of nanosilver through human skin was far less than through mouse skin. This result may be related to the kinds of skin, type of medium, and size and surface coating of nanosilver. Both results show that the nanosilver could indeed penetrate through the skin; the only difference between these results is in the permeation amount. Nanosilver will translocate to the circulatory system and eventually be distributed to target organs causing possible toxicity.<sup>40</sup>

The application potential of CS/GP/Ag hydrogel takes into consideration the indication of results in antibacterial activity, cytotoxicity, and skin permeation, as well as the CS/GP/Ag hydrogel necessary in order to have effective antibacterial activity and reduce toxicity to tissues for wound dressing applications. We recommend the CS/GP/Ag hydrogel prepared with DD88 CS, having an MW less than 200 kDa and containing 3 ppm of nanosilver.

## CONCLUSIONS

Manipulating the MW and DD of CS and the concentration of GP could lead to a gelation temperature for the CS/GP/Ag composite close to body temperature, causing a hydrogel to form by body heat. Gelation temperature and viscosity of the CS/GP/Ag hydrogel have an insignificant affect with different concentrations of nanosilver. The porous structure, water vapor transmission rate, and skin permeation of nanosilver for DD88 CS hydrogel are better than those for DD80 CS hydrogel. Both hydrogels with 6 and 12 ppm of nanosilver exhibited cytotoxicity on HS68 cells. The antibacterial activity of hydrogel increased with increased nanosilver concentration. The hydrogel exhibited antibacterial activity for *P. aeruginosa* and *S. aureus*, even without nanosilver. Hydrogel prepared with a lower MW CS presented higher antibacterial activity; therefore, in order to reduce the cytotoxicity of nanosilver, a newly formulated hydrogel could be proposed that offers similar antibacterial activity with lower MW CS and a lower concentration of nanosilver.

## ACKNOWLEDGMENTS

The authors wish to express their appreciation for the financial support from the National Science Council, ROC (NSC 97-2313-B-019-007-MY3, NSC 100-2313-B-019-004-MY3) and the Stone & Resource Industry R&D Center (Taiwan) [(SRDC-770-A1-56(99))].

## REFERENCES

- Harish Prashanth, K. V.; Tharanathan, R. N. *Trends Food Sci. Technol.* **2007**, *18*, 117.
- Honarkar, H.; Barikani, M. *Monatsh Chem.* **2009**, *140*, 1403.
- Jayakumar, R.; Prabakaran, M.; Nair, S. V.; Tamura, H. *Bio-technol. Adv.* **2010**, *28*, 142.
- Jayakumar, R.; Menon, D.; Manzoor, K.; Nair, S. V.; Tamura, H. *Carbohydr. Polym.* **2010**, *82*, 227.
- Tamura, H.; Furuike, T.; Nair, S. V.; Jayakumar, R. *Carbohydr. Polym.* **2011**, *84*, 820.
- Jayakumar, R.; Prabakaran, M.; Sudheesh Kumar, P. T.; Nair, S. V.; Tamura, H. *Biotechnol. Adv.* **2011**, *29*, 322.
- Jayakumar, R.; Chennazhi, K. P.; Sowmya, S.; Nair, S. V.; Furuike, T.; Tamura, H. *Int. J. Mol. Sci.* **2011**, *12*, 1876.
- Madhumathi, K.; Sudheesh Kumar, P. T.; Abhilash, S.; Nair, S. V.; Tamura, H.; Manzoor, K.; Nair, S. V.; Jayakumar, R. *J. Mater. Sci. Mater. Med.* **2010**, *21*, 807.
- Sudheesh Kumar, P. T.; Abhilash, S.; Manzoor, K.; Nair, S. V.; Tamura, H.; Jayakumar, R. *Carbohydr. Polym.* **2010**, *80*, 761.
- Chenite, A.; Chaput, C.; Wang, D.; Combes, C.; Buschmann, M. D.; Hoemann, C. D.; Leroux, J. C.; Atkinson, B. L.; Binette, E.; Selmani, A. *Biomaterials* **2000**, *21*, 2155.
- Kim, S.; Nishimoto, S. K.; Bumgardner, J. D.; Haggard, W. O.; Gaber, M. W.; Yang, Y. *Biomaterials* **2010**, *31*, 4157.
- Ruel-Gariépy, E. R.; Chenite, A.; Chaput, C.; Guirguis, C.; Leroux, J. C. *Int. J. Pharm.* **2000**, *203*, 89.
- Wu, J.; Wei, W.; Wang, L. Y.; Su, Z. G.; Ma, G. H. *Biomaterials* **2007**, *28*, 2220.
- Zan, J.; Chen, H.; Jiang, G.; Lin, Y.; Ding, F. *J. Appl. Polym. Sci.* **2006**, *101*, 1892.
- Zhao, Q. S.; Ji, Q. X.; Xing, K.; Li, X. Y.; Liu, C. S.; Chen, X. G. *Carbohydr. Polym.* **2009**, *76*, 410.
- Zhou, H. Y.; Chen, X. G.; Kong, M.; Liu, C. S. *J. Appl. Polym. Sci.* **2009**, *112*, 1509.
- Chenite, A.; Buschmann, M.; Wang, D.; Chaput, C.; Kandani, N. *Carbohydr. Polym.* **2001**, *46*, 39.
- Cho, J.; Heuzey, M. C.; Bégin, A.; Carreau, P. J. *Carbohydr. Polym.* **2006**, *63*, 507.
- Tsaih, M. L.; Tseng, L. Z.; Chen, R. H. *Polym. Degrad. Stab.* **2004**, *86*, 25.
- Tsaih, M. L.; Chen, R. H. *J. Appl. Polym. Sci.* **2003**, *88*, 2917.
- Molinaro, G.; Leroux, J. C.; Damas, J.; Adam, A. *Biomaterials* **2002**, *23*, 2717.
- Zhou, H. Y.; Chen, X. G.; Kong, M.; Liu, C. S.; Cha, D. S.; Kennedy, J. F. *Carbohydr. Polym.* **2008**, *73*, 265.
- Tsai, M. L.; Chang, H. W.; Yu, H. C.; Lin, Y. S.; Tsai, Y. D. *Carbohydr. Polym.* **2011**, *84*, 1337.
- Jain, J.; Arora, S.; Rajwade, J. M.; Omray, P.; Khandelwal, S.; Paknikar, K. M. *Mol. Pharm.* **2009**, *6*, 1388.
- Ong, S. Y.; Wu, J.; Moochhala, S. M.; Tan, M. H.; Lu, J. *Biomaterials* **2008**, *29*, 4323.
- Wu, P.; Fisher, A. C.; Foo, P. P.; Queen, D.; Gaylor, J. D. *Biomaterials* **1995**, *16*, 171.
- Lin, C. C.; Lin, H. Y.; Chen, H. C.; Yu, M. W.; Lee, M. H. *Food Chem.* **2009**, *116*, 923.
- Kong, H.; Jang, J. *Chem. Commun.* **2006**, 3010.
- Chen, R. H.; Chen, W. Y.; Wang, S. T.; Hsu, C. H.; Tsai, M. L. *Carbohydr. Polym.* **2009**, *78*, 902.
- Chen, R. H.; Lin, J. H.; Yang, M. H. *Carbohydr. Polym.* **1994**, *24*, 41.
- Chen, R. H.; Tsaih, M. L.; Lin, W. C. *Carbohydr. Polym.* **1996**, *31*, 141.
- Hwang, C.; Rha, C. K.; Sinskey, A. J. In *Chitin in Nature and Technology*; Muzzarelli, R. A. A.; Jeuniaux, C.; Gooday, G. W., Eds.; Plenum Press: New York, **1986**; p 389.
- Pei, H. N.; Chen, X. G.; Li, Y.; Zhou, H. Y. *J. Biomed. Mater. Res. A* **2008**, *85*, 566.
- Lamke, L. O.; Nilsson, G. E.; Reithner, H. L. *Burns* **1977**, *3*, 159.
- Wu, P.; Nelson, E. A.; Reid, W. H.; Ruckley, C. V.; Gaylor, J. D. *Biomaterials* **1996**, *17*, 1373.
- Tsai, G. J.; Tsai, M. T.; Zhong, M. Z.; Lee, J. M. *J. Food Prot.* **2006**, *69*, 2168.
- Dutta, P. K.; Tripathi, S.; Mehrotra, G. K.; Dutta, J. *Food Chem.* **2009**, *114*, 1173.
- Xie, F.; Li, Q. F.; Gu, B.; Liu, K.; Shen, G. X. *Microsurgery* **2008**, *28*, 471.
- Zhao, Q. S.; Cheng, X. J.; Ji, Q. X.; Kang, C. Z.; Chen, X. G. *J. Sol-Gel Sci. Technol.* **2009**, *50*, 111.
- Ahamed, M.; ALSalhi, M. S.; Siddiqui, M. K. *J. Clin. Chim. Acta.* **2010**, *411*, 1841.
- Larese, F. F.; D'Agostin, F.; Crosera, M.; Adami, G.; Renzi, N.; Bovenzi, M.; Maina, G. *Toxicology* **2009**, *255*, 33.